Water–Ions Induced Nanostructuration of Hydrophobic Polymer Surfaces

Igor Siretanu,[†,‡] Jean Paul Chapel,[†] and Carlos Drummond[†,*]

[†]Université de Bordeaux, Centre de Recherche Paul Pascal, UPR8641 CNRS, Avenue Schweitzer, 33600 Pessac Cedex, France, and [‡]Laboratoire de Chimie des Polymères Organiques, CNRS, Université Bordeaux 1, 33607 Pessac Cedex, France

ABSTRACT When hydrophobic surfaces are in contact with water in ambient conditions a layer of reduced density is present at the interface, preventing the intimate contact between the two phases. Reducing the extent of this layer by degassing the water can have remarkable implications for the interaction between the two phases. The enhanced proximity between a hydrophobic polymer film and an aqueous solution can induce a self-assembled nanostructure on the solid surface through the development of an electro-hydrodynamic instability, due to the adsorption of the water–ions (hydronium and hydroxyl) at the interface. The self-assembled structure spontaneously relaxes back to the original flat morphology after few weeks at room temperature. This instability and the self-assembled structure are controlled by the hydrophobic surface charge, which is determined by the pH of the aqueous phase, and by the amount of gas dissolved. This effect can be easily adjusted to modify different hydrophobic polymeric substrates at the submicrometer level, opening pathways for producing controlled patterns at the nanoscale in a single simple waterborne step.

KEYWORDS: nanopatterning · polymer materials · thin films · water/polymer interface

When water is in contact with air in standard conditions, oxygen and nitrogen are dissolved in concentrations of 0.2 mM and 0.5 mM, respectively. It has been shown in the past that reducing the concentration of the dissolved gases may affect several interfacial properties. Despite of the fact that oil and water do not mix, spontaneous emulsification of hydrocarbons occurs after water degassing.[1−3] Colloids stability,[4] the range of the hydrophobic interaction,[5] the conductivity of salt solutions,[6] the efficiency of flotation process,[7] and the slippage boundary conditions in flowing water[8] are all affected by the amount of gas in solution.

An extensive body of research has been devoted to the study of most of these problems. Particularly, the description of the intimate contact between water and hydrophobic surfaces has been the subject of controversial debates for the past few decades, probably due to its central role in many natural phenomena and technological applications. It has been suggested than a region of reduced density may be present at the interface between water and hydrophobic surfaces, although the nature of this depleted layer remains controversial. A number of scanning probe microscopy studies reporting the presence of soft nanometric objects near hydrophobic surfaces in water have been published[9−13] after their existence was suggested 15 years ago.[14] Indeed, some reports of the nucleation of micrometric-size bubbles on hydrophobic surfaces were published long before.[15] However, no explanation for the very existence of long-lasting nanobubbles that considers the large Laplace pressure inside them has been advanced. Some researchers have even suggested that the observed nanobubbles in scanning probe experiments are a consequence of confinement effects or tip–substrate interaction.[16,17] On the contrary, a detailed X-ray reflectivity study on hydrophobic substrates, while supporting the existence of a depleted water layer by the interface, argued against the existence of micro- or nanobubbles.[18] Independent reflectivity experiments have also evidenced the presence of a layer of reduced water density near hydrophobic surfaces with an extension determined by the concentration of dissolved gases.[19−22] However, some ellipsometric[23] and neutron reflectivity studies[24] failed to observed the existence of a water depletion gap. Despite of the long list of seemingly contradictory results, consensus is slowly emerging around the idea that a boundary layer of reduced density is indeed present when water is nearby a hydrophobic surface, although its nature is yet to be firmly established.[25,26]

In this work we explore the effect of dissolved gases in the interface between water solutions and several hydrophobic

* Address correspondence to drummond@crpp-bordeaux.cnrs.fr.

Received for review December 22, 2010 and accepted March 24, 2011.

Published online March 24, 2011
10.1021/nn103564e

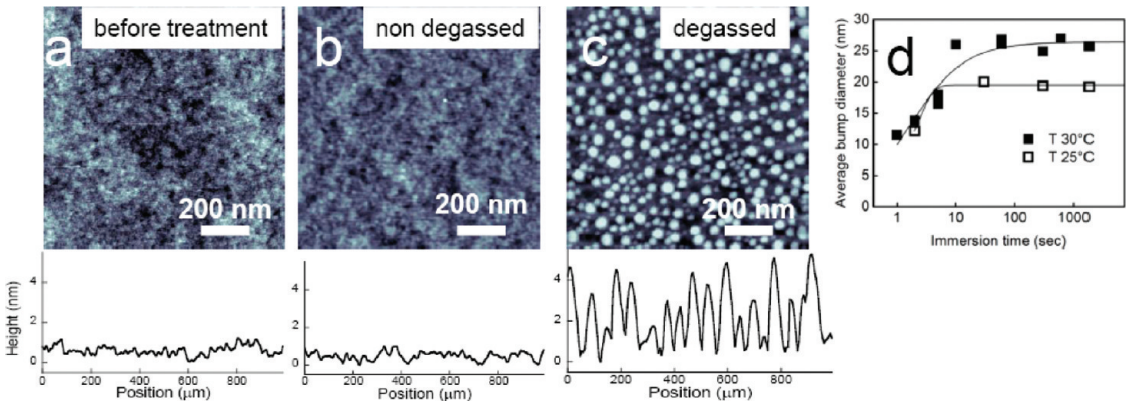

Figure 1. Tapping mode AFM micrographs (1 μm $\times$ 1 μm height) taken in air of 300 nm thick, 250 kDa polystyrene films as prepared (spin-coated) (a); after exposure to a nondegassed (b) and degassed (c) solution of nitric acid in double distilled water at pH 1.5 and room temperature. A typical height profile for each condition is presented. The presence of asperities of regular nanometric size is clearly observed on the surface exposed to the degassed solution for 5 min. On the contrary, no modification was detected when an identical film was exposed to the same solution under identical conditions (or much longer times) before removing the dissolved gases. XPS tests showed that no chemical modification of the films has occurred (see Supporting Information). (d) Temporal evolution of bump diameter with immersion time at two different temperatures.

polymers. In particular, we report how this interface is modified by the degassing of the aqueous phase, showing the influence of dissolved gases and ions present in the water on the interaction between water and a hydrophobic surface. Previously published results have evidenced how the morphology of hydrophobic surfaces can be severely modified in the presence of nanobubbles.[27−29] We show here how this effect depends strongly on the amount of gas dissolved in the aqueous phase, and more importantly on the nature of the ions dissolved in the water. In addition, the results described in this paper clearly evidence the presence of a layer of enhanced mobility at the outermost surface of glassy polystyrene films enabling a possible surface reconstruction at temperatures well below the glass transition temperature, T_g; a controversial and debated topic nowadays.[30] Otherwise, no surface structuration would be possible.

RESULTS AND DISCUSSION

We have used spin coating to produce smooth 300 nm thin films of polystyrene PS of five different molecular weights above and below the entanglement length (7, 59, 160, 250, and 500 kDa) on surfaces of freshly cleaved mica, glass, or polished silanized silicon wafers. The PS films were then exposed to aqueous solutions, dried with a gentle flow of nitrogen gas, and studied by AFM in air. While no noticeable change of morphology was observed when the films were exposed to an aqueous solution in equilibrium with air, nanopatterns appeared in the surfaces after few minutes of exposure to degassed water solutions, as can be observed in Figure 1. Similar results were obtained for all the polymers investigated. The characteristic size and density of the self-assembled nanostructure are mainly determined by the pH and composition of the aqueous phase and the temperature. The surface structuration has no effect on the wettability of the surfaces: the contact angle of water on the substrate is not changed by the process. However, the hydrophobicity of the surface seems to determine the outcome of the process: the structuration of the film is not observed if the polymer surface is rendered hydrophilic (θ = 30°) before the water treatment by partial UV-oxidation (5 min irradiation under an Hg vapor lamp, UVOCS). This treatment did not significantly change the thickness or the morphology of the film, as verified by ellipsometry and AFM. It is known that the UV oxidation reduces the water contact angle on the surface by chain scission and partial oxidation of the PS, but it also enables cross-linking between polymer chains.[31] To discard the possible effect of reduced PS mobility by cross-linking, the film was rendered again hydrophobic by heating it at 70 °C during 10 h under dry conditions (the water contact angle θ after this treatment was 85°). This step allowed the reconstruction of the film *via* conformational changes or chain diffusion reducing the interfacial free energy.[32] Subsequent exposure to degassed acid water effectively provoked the structuration of the film. The results of these tests are presented as Supporting Information.

Two remarkable conclusions can be drawn from this interesting effect. First, the interaction between the aqueous phase and the hydrophobic substrate is fundamentally modified by the gases dissolved which shelter the hydrophobic substrate from the aqueous phase. Second, there is a mobile surface layer on the polymer which can be restructured under external stimuli, even though we are working at temperatures largely below the glass transition temperature T_g of PS. This indicates that macromolecular chains near the interface have properties which deviate significantly from their bulk counterparts. Indeed, no structuration was observed in films of UV cross-linkable PS after UV

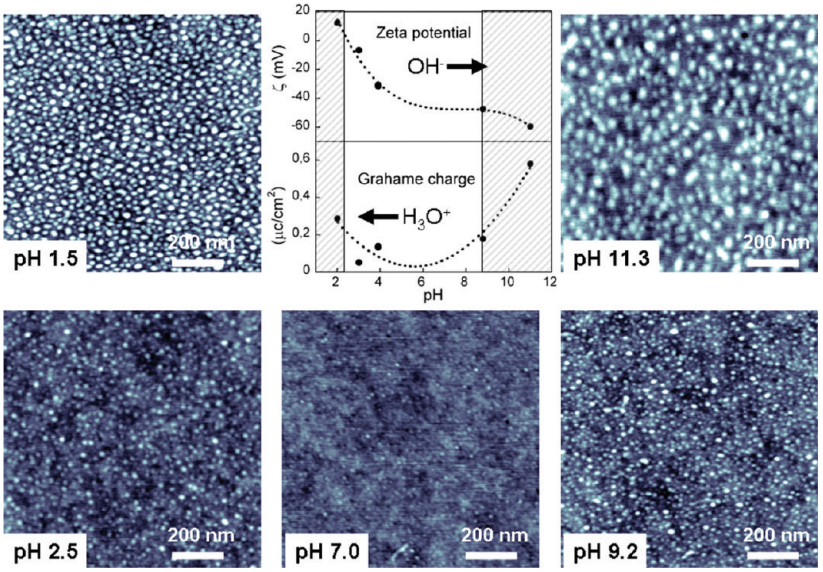

Figure 2. Tapping mode AFM micrographs (1 μm $\times$ 1 μm height) taken in air of 300 nm thick, 250 kDa PS films treated with degassed water at different pH values, varied with HNO_3 and NaOH. The graphs show the measured zeta potential and calculated charge density of each substrate. Structuration is observed at pH values in the dashed zones. The modification of the polymer surface in contact with degassed water is determined by the pH of the solution: while relatively large self-assembled blobs are observed at low and high pH values, their size and density get substantially smaller under neutral conditions.

curing, evidencing the importance of surface mobility. Recently, by studying the relaxation of nanometric deformations on films of PS, Fakhraai and Forrest[30] showed that the mobility of polymer chains is dramatically accelerated nearby the surfaces with respect to the bulk. Although it is still poorly understood, several explanations have been advanced for this enhanced dynamic, related to the reduced entanglement density, enrichment of chain ends, and increased free volume for the polymer molecules at the surface.[30]

As can be observed in Figure 2, the characteristic size of the observed patterns is modified by the pH of the degassed water. More important modifications are observed at high or low pH values. Interestingly, streaming potential measurements suggest ionic adsorption on the surfaces at the same conditions. In agreement with previously reported results,[33] we observed a strong variation of the zeta potential of the hydrophobic polymer surfaces with pH. The observed surface structuration seems to correlate well with the values of the surface charge density as derived from the measured zeta potential of the surfaces using the Grahame equation:[34,35] the higher the value of the surface charge density, the larger is the effect of the aqueous phase on the structure of the polymer surface. This striking result seems to be largely independent of the ionic strength: while the structuring effect of degassed solutions of sodium chloride, nitrate, or perchlorate 0.1 M is not much larger than the one of water at neutral pH, the structure obtained at pH 1.5 was almost independent of the presence of $NaNO_3$ in solution at concentrations up to 0.2 M (Supporting Information).

The subsequent evolution of the self-assembled structure is determined by the environmental conditions. As can be observed in Figure 3, the structure disappears after the structured surface is annealed at 95 °C for a few hours. Nevertheless, these patterns reappear if the surface is exposed again to degassed aqueous solutions. The patterns also relax under solvent annealing: after exposure to toluene vapor for 1 h most of the structuration is removed. Indeed, the surface of the film slowly relaxes back to the original smooth condition even when the films are conserved in air at room temperature. We observed a faster evolution of the films of PS of lower molecular weights; a complete report of this feature will be presented in a forthcoming publication.

There is an enormous difference in the time scale of formation and relaxation of the nanostructures. While a well-developed structured layer is formed after a few minutes of contact between the degassed water solution and the film, the typical time of relaxation of the structure is few weeks, in agreement with a recently published study of temporal evolution of nanoindented PS substrates.[30] As can be observed in Figure 3, two different mechanisms govern the temporal evolution of the nanostructured layers. First, smaller size blobs disappear at expenses of larger ones which increase further in size (*e.g.*, the region indicated by the arrows) evidencing the mobility of the polymer chains at the surface. This process, which coarsens the size distribution of the asperities on the surface, suggests the occurrence of surface Ostwald ripening. Second, a slow relaxation of the measured blobs is detected. This relaxation is driven by the Laplace

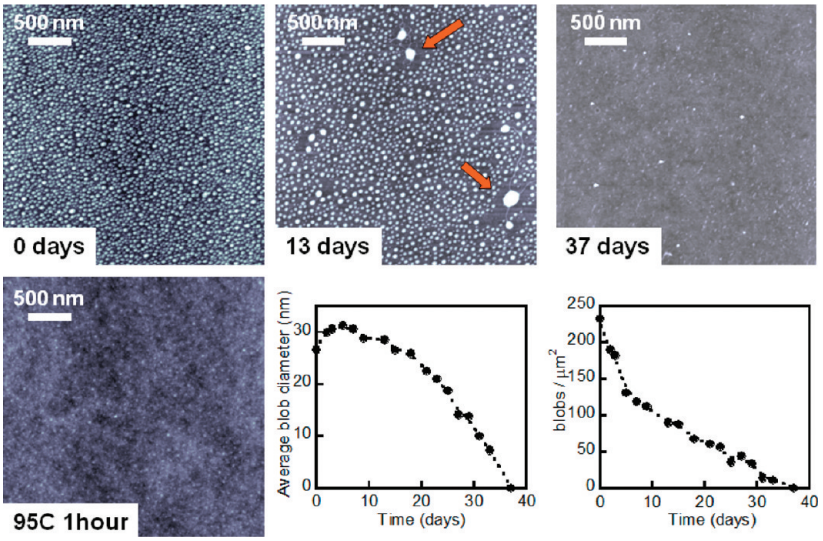

Figure 3. AFM micrographs (3 μm $\times$ 3 μm height) measured in air on a film that has been previously in contact with degassed water at pH 1.5 at different times after water exposure, as indicated. The self-assembled nanostructure on the polymer surface is not at thermodynamic equilibrium. One month after the nanostructuration was induced most of the asperities on the film have already relaxed at room temperature, and the film recovers its original smooth morphology. The relaxation of the structure is greatly accelerated by increasing the temperature.

pressure on the formed blobs, $\Delta P = 2\gamma/R$. The spontaneous relaxation of the structure confirms that the process is not a consequence of irreversible plastic deformation of the films; it is due to the presence of a zone of enhanced mobility on top of the polymer surface able to deform and reshape.

What is the driving force for the observed nanostructuration? Usually, in order to describe the interface between an aqueous solution and a charged surface, one considers the effect of surface charges due to surface ionization or ionic adsorption on the ionic distribution in the liquid phase. This distribution determines the properties of the material. It seems that a change of paradigm is necessary to understand the phenomena reported in this work. The essence of the problem can be captured through the following question: *what is the influence of the water structure and the ionic distribution on the hydrophobic surface?* It has long being recognized that pristine water/oil interfaces can become charged.[36,37] It is becoming apparent from experiments and simulations that the density of ions in water solutions close to hydrophobic objects is not uniform: some ions are preferentially attracted to the interface.[38,39] The adsorption of water−ions on hydrophobic surfaces has been evoked to explain phenomena as diverse as the electrophoretic mobility of hydrophobic objects,[38,39] the nanotube catalyzed etching of silicon dioxide,[40] or the electrochemical behavior of graphene.[41] Different mechanisms—entropy changes,[42] ionic asymmetry,[43] ionic polarizability,[44] and ionic-induced decrement of water polarization fluctuations[38,39]—have been evoked to explain this ionic distribution which defies straightforward electrostatic considerations: ions should strongly partition into the higher dielectric constant aqueous phase. Despite of the debates around this subject, consensus seems to be emerging around the idea that the interfacial density of hydroxyl or hydronium ions increases nearby water-hydrophobic interfaces, with the respective amount determined by pH.[38,39] This explains why the charge of hydrophobic surfaces in water strongly changes with the pH of the aqueous phase but is less sensitive to the presence of other ions, in agreement with previous experimental and theoretical studies of the physisorption of water ions to hydrophobic surfaces.[38,39]

The strong adsorption of these ions at the interface is probably at the origin of the phenomena reported here: they originate an electric field which polarizes the polymer layer and leads to its rearrangement. It has already been shown by several groups that it is possible to pattern a polymer liquid film by applying an electric field strong enough to induce an electrohydrodynamic instability.[45] Surface waves can appear at the interface between water and an immiscible liquid from the interplay between the Laplace and the electrostatic pressures; no other force needs to be considered for the films studied here, given that they are sufficiently thick so that the effect of dispersive forces is unimportant,[46] and thin enough as to make the influence of gravity irrelevant. This simple picture requires the ions to be very close to the interface, or the dielectric constant of the media between the ions and the polymer film to be significantly reduced: otherwise a repulsive "image" force between the ions and the low dielectric constant polymer film should be expected,[47] which is inconsistent with the structuration reported here.

To determine the effect of the ionic distribution on the polymer films, precise details of the amount and

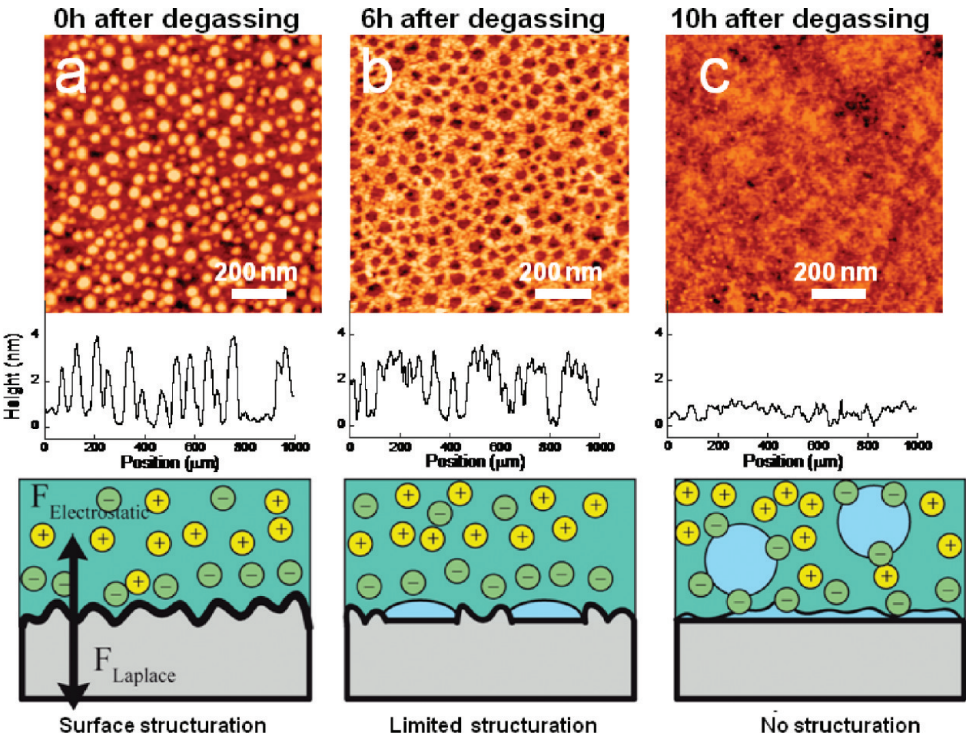

Figure 4. The amount of dissolved gas determines the nature and extent of the surface structuration. PS films (300 nm thick, 250 kDa) were immersed for 10 min in water at pH 1.5 and then studied by AFM in air. Before treating the surfaces, the aqueous solution was in contact with air during different periods of time after degassing as indicated, to change the amount of gas dissolved. (a) Shortly after degassing the preferential adsorption of ions at the water/polymer interface is likely to be responsible for the observed self-assembled nanostructure. Increasing amounts of gas in the solution move the ions away from the polymer surface limiting the structuration below the bubbles (b), or the low density layer (c). This process argues in the direction of supporting three controversial issues: (i) the presence of a low density layer at the interface between a hydrophobic surface and water with dissolved air, (ii) the preferential adsorption of hydroxyl and/or hydronium ions on hydrophobic surfaces, (iii) the presence of a zone of enhanced mobility at the outermost surface of a PS film.

location of the ions in the interface are necessary, which is out of reach even for the largest scale simulations. However, we can make a crude estimation of the electric field in the polymer film by assuming that a certain density of ions is preferentially placed in the water nearby the polymer/water interface. An electric field on the polymer surface of the order of 10^7 V/m can be calculated from the surface charge values presented in Figure 2.[48] The electrostatic pressure induced by the field at the polymer−water interface can be estimated as described by Landau and Lifshitz,[47] if the variation of the dielectric constant of the polymer is not taken into account.[49] A value of the order of 0.1 MPa is obtained, largely inferior to the yield stress of PS (30 MPa).[30] The evolution of the polymer surface will then be determined by the competition between the destabilizing effect of the field and the Laplace pressure, which damps the surface fluctuations. The macroscopic description of the problem of the deformation of a viscous liquid with a uniform surface charge density has been reported before.[50] If we estimate the wavelength of the fastest growing mode in our films by using the dispersion relation deduced by Killat[50] (Supporting Information) values between 15 and 150 nm are obtained, in agreement with the structures presented in Figures 1−2. The kinetic of formation and relaxation of the waves will be determined by the viscosity of the liquid and the interfacial tension. From the same dispersion relationship, a viscosity of the order of 100 MPa·s can be estimated for the mobile layer of the PS films, orders of magnitude lower than the value expected for PS at temperatures below T_g. This macroscopic description cannot be applied if the density of charges at the interface is too low. In that case a description at the molecular level which takes into account the discreteness of the matter is likely to be necessary. This description cannot be built based on the finding reported in this work only. Detailed molecular modeling of the present systems will probably be necessary to reach a complete understanding of the reported phenomena. Nevertheless, it seems apparent that the driving force for the structuration is the preferential presence of water ions at the water/polymer interface. The electric field on the polymer depends critically on the density of charges and notably on the separation between the charges and the interface. Displacing the position of the charges by a fraction of a nanometer entails a dramatic reduction of the electric field on the polymer, leading to the disappearance of the nanostructuration. This explains

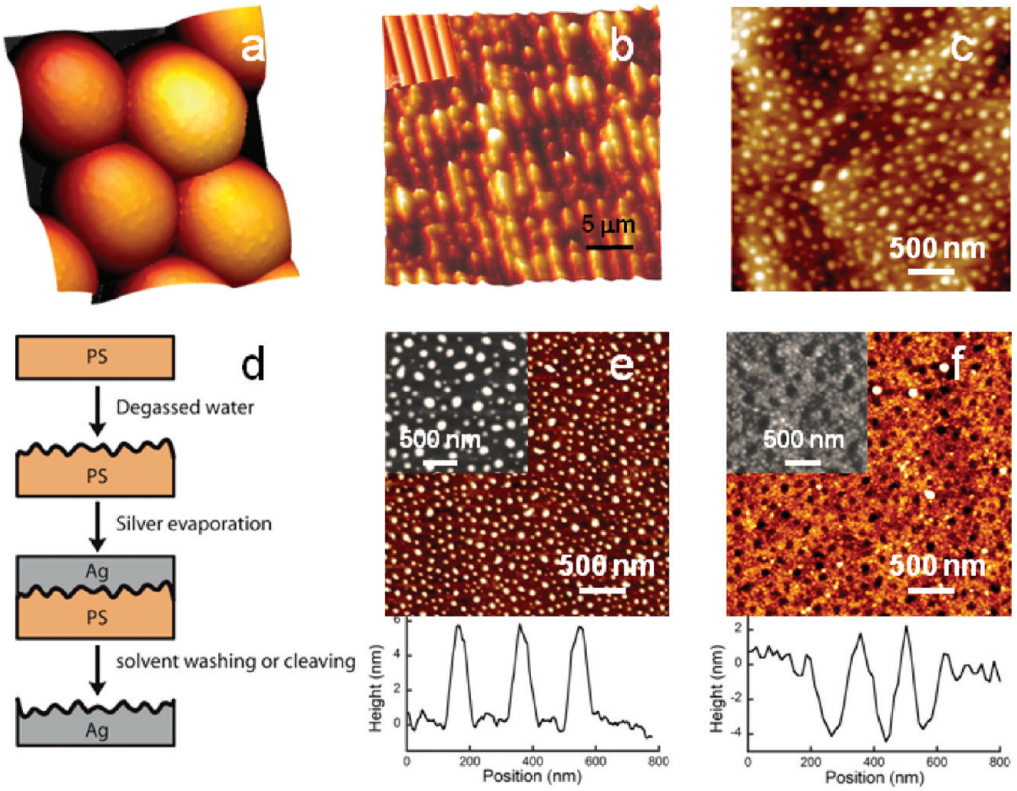

Figure 5. AFM micrographs taken in air show that the surface nanostructuration was also observed in (a) a layer of PS latex (radii 0.2 μm) deposited by dip-coating from a concentrated aqueous solution (10 g/L) on top of a smooth mica surface, (b) in bulk PS partially protected by a sinusoidal microwrinkled PDMS-stamp (right; λ = 2 μm; see inset) and (c) a film of semicrystalline polyethylene. The polymer modified surfaces can also be used as a template to pattern metallic films as outlined in panel d. Evaporating a 250 nm thick silver film on a structured PS film and removing the polymer film after gluing the stack onto a convenient substrate, allows production of a metallic film of controlled surface structure (e, f). For example, a PS film with nanoholes (*e.g.*, Figure 4, central panel) can be used as a template to produce a metallic surface with bumps of controlled size (e).

why the presence of a very thin layer of reduced density deeply modifies the interaction between both phases.

Indeed, it is very revealing to explore the effect of the amount of gas dissolved on the structuration process. As can be observed in Figure 4, the size of the observed bumps is larger at short times after degassing; 10 h after degassing water has regained its equilibrium with the atmosphere, and no structuring effect is detected. On the contrary, at intermediate times a seemingly different structuration effect is observed: the contact with the aqueous phase induces the formation of a regular array of shallow holes/rims in the polymer film, with a typical size of 30 nm and depth of 2 nm. The formation of a similar pattern has been reported by Wang and co-workers.[27] They suggested that the high tensile stress inside of nanobubbles on the hydrophobic surface is responsible for the appearance of "nanoindents". However, we do not observe this effect in neutral water: only at sufficiently low or high pH values are these "nanoindents" present. The ensemble of our results suggests the following scenario (Figure 4). At low concentration of dissolved gas, the preferential adsorption of ions at the interface generates an attractive force on the polymer molecules at the surface inducing the formation of bumps. At higher gas concentrations a layer of nanobubbles nucleate on the surface. Small bumps are still formed in the region between or at the rim of the nanobubbles, where the air thickness is thin enough; we do not need to evoke a different mechanism to explain the different observed morphologies. In all cases, the thickness of the structured region (between 2 and 3 nm) is consistent with recent reports of the presence of a thin mobile layer on the surface of glassy PS films.[30,51] At higher gas concentration larger bubbles or even a continuous low-density layer is present at the water−polymer interface and no structuration effect is detected.

The procedure described here may be of interest for producing controlled nanostructured structures on flat, nonplanar, or hollow hydrophobic substrates in a single simple step allowing an easy and precise control of the nanopatterns produced.[52] Some realizations of this idea are presented in Figure 5: the nanostructuration of a monolayer of PS microspheres—a substrate that would be impossible to pattern with conventional lithographic techniques—or the selective patterning of a PS substrate partially protected by a PDMS mask

were performed in a simple waterborne step. The obtained patterned polymer surfaces can also be replicated by metal thermal evaporation to produce nanostructured metallic films with holes or asperities of controlled size, as illustrated in Figure 5d–f. After deposition of a sufficiently thick metal layer, the polymer layer can be cleaved or dissolved away. This procedure allows an efficient and precise control of the metallic surface structure, with possible applications in materials science and photonics. The roughness of polydimethylsiloxane (PDMS) surfaces can be tuned by this technique if the PDMS is treated while cross-linking, which may be of interest for microfluidic applications. Nanostructuration was also observed on a bulky PS substrate made from molten PS pellets sandwiched between two smooth glass slides. These results rule out the influence of the inorganic substrate and/or the thickness of the PS layer on the nanostructuration phenomena. We have observed that substrates of poly(methyl methacrylate) (PMMA), PS in the form of colloidal spheres and bulk, and semicrystalline films of polyethylene (PE) are also prone to be structured by this technique (Figure 5c). We believe that these phenomena are relevant for the interface between water and any hydrophobic object, and should be considered in the description of processes as diverse as protein folding, surfactant aggregation, friction or adhesion. It may find applications in many different scientific and technological fields like nanolithography, microfluidics or flexible electronics.[53]

METHODS

Materials. Polystyrene (PS) of five different molecular weights (7, 59, 160, 250, and 500 kDa) were investigated. PS of 500 kg/mol (T_g = 103 °C) and 59 kg/mol (T_g = 102 °C) were obtained from Sigma-Aldrich. PS of 250 kg/mol (T_g = 103 °C) was obtained from ACROS Organics. Cross-linkable[54] PS of 160 kg/mol (poly[styrene-*co*-(4-azidomethylstyrene)) was a generous gift of Dr. Eric Drockenmuller. PS of 7 kg/mol (T_g = 90 °C) synthesized by ATRP, was a gracious gift from Dr. Antoine Bousquet. PS latex (suspension of PS spheres of radius 400 nm) was obtained from Polyscience

Film Preparation. The PS films were obtained by spin coating solutions of the polymer in toluene 5% w/w onto silicon wafers or freshly cleaved mica surfaces unless otherwise indicated. To increase the adhesion of the polymer film on the substrates and to avoid the penetration of water between the film and the substrates, in some cases the silicon wafers were coated with a silane layer by a 2 h exposure to a solution of octadecyltrimethoxysilane (abcr Specialty Chemicals) in toluene. Identical results were obtained in the absence of this primer silane layer. The cast films were annealed at 95 °C for 12 h to remove the residual solvent and release any mechanical stress built up during the spin coating process. Similar results were obtained with films annealed at 150 °C for 6 h.

Films of cross-linkable PS were produced by spin coating a solution of the polymer in toluene 0.4% w/w. Cross-linking of the PS film was performed by irradiating the film with ultraviolet (UV) light (300–360 nm) during 1 h, as described in ref 54.

Film Characterization. The thickness of the films was determined by ellipsometry (Nanofilm); roughness and morphology were assessed by atomic force microscopy in tapping mode (multimode and Icon, Veeco). The films were also characterized by water contact angle (IDC Concept) and streaming potential measurements (CAD). Extremely smooth films of thickness 300 nm, with a rms roughness smaller than 0.5 nm were typically obtained. The contact angle of water on the films was around 90° with very small hysteresis. Most of the results presented in this work were obtained with 250 kDa PS chains on 300 nm thick films on silanized silicon wafers, although qualitatively analogous observations were made with the other polymer samples.

Water Degassing and Film Treatment. Millipore water with a conductivity of 18 MΩ cm^{-1} was used for the solution preparation. The pH of the aqueous phase was adjusted by adding small amounts of NaOH (Prolabo) or nitric acid (Aldrich) as necessary. Similar results were obtained by using HCl (Aldrich) or KOH (Aldrich). Carefully cleaned Teflon bar stirrers were introduced in the solutions to be degassed to induce the nucleation of gas bubbles. The solutions were subjected to agitation under a pressure of 0.2 mbar for 2 h. The appearance of macroscopic bubbles in the aqueous phase was observed only during the first 30 min of degassing. After the degassing is finished, the air pressure on the flask was gently increased back to atmospheric pressure. The degassed solutions were put right away in contact with the polymer surfaces for a few minutes after stopping the pumping, unless otherwise indicated. The PS films were then dried with a gentle flow of nitrogen gas.

Zeta Potential. An aqueous solution with the right pH and ionic strength was driven through a channel bounded by the surfaces of interest and the streaming potential, Φ_{str}, was measured at different pressure drop values, Δp. The zeta potential, ζ, was calculated from the slope of the linear curves of streaming potential as a function of Δp by[55]

$$\zeta = \frac{\Phi_{str}\eta k_L}{\varepsilon_w \varepsilon_0 \Delta p}$$

where ε_w is the relative permittivity of the solution, ε_o is the electric permittivity of vacuum, and η and k_L are the viscosity and conductivity of the solution

Grahame Equation. The Grahame equation[34,35] based on the Gouy–Chapman theory relates the surface charge density σ to the surface potential ψ_0. This equation proceeds readily from the electroneutrality condition: the total charge, that is, the surface charge plus the charge of the ions in the whole double layer, must be zero. It follows:

$$\sigma = \sqrt{8c_0\varepsilon_w\varepsilon_0 k_B T}\,\sinh\left(\frac{e\psi_0}{2k_B T}\right)$$

where c_0 is the salt bulk concentration, e is the electronic charge, T is the temperature, and k_B is the Boltzmann constant.

In the case of a low surface potential, sinh(x) reduces to x and leads to the simple relationship:

$$\sigma = \frac{\varepsilon_w \varepsilon_0 \psi_0}{\kappa^{-1}}$$

where κ^{-1} is the Debye screening length.

Acknowledgment. We acknowledge Christine Labrugere for her assistance with the XPS measurements.

Supporting Information Available: AFM micrographs showing the temporal evolution of the film while structuration, the influence of water wettability and solution pH on the nanostructuration. XPS analysis of selected samples after water treatment. Derivation of the instability characteristic length[50] applied to the system studied in this paper. This material is available free of charge *via* the Internet at http://pubs.acs.org.

REFERENCES AND NOTES

1. Pashley, R. M. Effect of Degassing on the Formation and Stability of Surfactant-Free Emulsions and Fine Teflon Dispersions. *J. Phys. Chem. B* **2003,** *107*, 1714–1720.
2. Beattie, J. K.; Djerdjev, A. M. The Pristine Oil/Water Interface: Surfactant-Free Hydroxide-Charged Emulsions. *Angew. Chem., Int. Ed.* **2004,** *43*, 3568–3571.
3. Maeda, N.; Rosenberg, K. J.; Israelachvili, J. N.; Pashley, R. M. Further Studies on the Effect of Degassing on the Dispersion and Stability of Surfactant-Free Emulsions. *Langmuir* **2004,** *20*, 3129–3137.
4. Snoswell, D. R. E.; Duan, J.; Fornasiero, D.; Ralston, J. Colloid Stability and the Influence of Dissolved Gas. *J. Phys. Chem. B* **2003,** *107*, 2986–2994.
5. Meyer, E. E.; Lin, Q.; Israelachvili, J. N. Effects of Dissolved Gas on the Hydrophobic Attraction between Surfactant-Coated Surfaces. *Langmuir* **2005,** *21*, 256–259.
6. Pashley, R. M.; Rzechowicz, M.; Pashley, L. R.; Francis, M. J. Degassed Water Is a Better Cleaning Agent. *J. Phys. Chem. B* **2005,** *109*, 1231–1238.
7. Dai, Z.; Fornasiero, D.; Ralston, J. Influence of Dissolved Gas on Bubble−Particle Heterocoagulation. *J. Chem. Soc., Faraday Trans.* **1998,** *94*, 1983–2987.
8. Cottin-Bizonne, C.; Cross, B.; Steinberger, A.; Charlaix, E. Boundary Slip on Smooth Hydrophobic Surfaces: Intrinsic Effects and Possible Artifacts. *Phys. Rev. Lett.* **2005,** *94*, 056102.
9. Mahnke, J.; Stearnes, J.; Hayes, R. A.; Fornasiero, D.; Ralston, J. The Influence of Dissolved Gas on the Interactions between Surfaces of Different Hydrophobicity in Aqueous Media Part I. Measurement of Interaction Forces. *Phys. Chem. Chem. Phys.* **1999,** *1*, 2793–2798.
10. Ishida, N.; Inoue, T.; Miyahara, N.; Higashitani, K. Nanobubbles on a Hydrophobic Surface in Water Observed by Tapping-Mode Atomic Force Microscopy. *Langmuir* **2000,** *16*, 6377–6380.
11. Tyrrell, J. W. G.; Attard, P. Images of Nanobubbles on Hydrophobic Surfaces and Their Interactions. *Phys. Rev. Lett.* **2001,** *87*, 176104.
12. Yang, J.; Duan, J.; Fornasiero, D; Ralston, J. Very Small Bubble Formation at the Solid−Water Interface. *J. Phys. Chem. B* **2003,** *107*, 6139–6147.
13. Holmberg, M.; Kuhle, A.; Garnaes, J.; Morch, K. A.; Boisen, A. Nanobubble Trouble on Gold Surfaces. *Langmuir* **2003,** *19*, 10510–10513.
14. Attard, P. Bridging Bubbles between Hydrophobic Surfaces. *Langmuir* **1996,** *12*, 1693–1695.
15. Newton Harvey, E.; Barnes, D. K.; McElroy, W. D.; Whiteley, A. H.; Pease, D. C. Removal of Gas Nuclei from Liquids and Surfaces. *J. Am. Chem. Soc.* **1945,** *67*, 156–157.
16. Steitz, R.; Gutberlet, T.; Hauss, T.; Klosgen, B.; Krastev, R.; Schemmel, S.; Simonsen, A. C.; Findenegg, G. H. Nanobubbles and Their Precursor Layer at the Interface of Water against a Hydrophobic Substrate. *Langmuir* **2003,** *19*, 2409–2418.
17. Yakubov, G. E.; Butt, H.-H.; Vinogradova, O. I. Interaction Forces between Hydrophobic Surfaces. Attractive Jump as an Indication of Formation of "Stable" Submicrocavities. *J. Phys. Chem. B* **2000,** *104*, 3407–3410.
18. Mezger, M.; Schöder, S.; Reichert, H.; Schröder, H.; Okasinski, J.; Honkimäki, V.; Ralston, J.; Bilgram, H.; Roth, R.; Dosch, H. Water and Ice in Contact with Octadecyl−Trichlorosilane Functionalized Surfaces: A High Resolution X-ray Reflectivity Study. *J. Chem. Phys.* **2008,** *128*, 244705.
19. Doshi, D. A.; Watkins, E. B.; Israelachvili, J. N.; Majewski, J. Reduced Water Density at Hydrophobic Surfaces: Effect of Dissolved Gases. *Proc. Natl. Acad. Sci. U.S.A.* **2005,** *102*, 9458–9462.
20. Mezger, M.; Sdelmeier, F.; Horinek, D.; Reichert, H.; Pontoni, D.; Dosch, H. On the Origin of the Hydrophobic Water Gap: An X-ray Reflectivity and MD Simulation Study. *J. Am. Chem. Soc.* **2010,** *132*, 6735–6741.
21. Jensen, T. R.; Østergaard-Jensen, M.; Reitzel, N.; Balashev, K.; Peters, G. H.; Kjaer1, K.; Bjørnholm, T. Water in Contact with Extended Hydrophobic Surfaces: Direct Evidence of Weak Dewetting. *Phys. Rev. Lett.* **2003,** *90*, 086101.
22. Poynor, A.; Hong, L.; Robinson, I. K.; Granick, S.; Zhang, Z.; Fenter, P. A. How Water Meets a Hydrophobic Surface. *Phys. Rev. Lett.* **2006,** *97*, 266101.
23. Mao, M.; Zhang, J.; Yoon, R.-H.; Ducker, W. A. Is There a Thin Film of Air at the Interface between Water and Smooth Hydrophobic Solids?. *Langmuir* **2004,** *20*, 1843–1849.
24. Seo, Y.-S.; Satija, S. No Intrinsic Depletion Layer on a Polystyrene Thin Film at a Water Interface. *Langmuir* **2006,** *22*, 7113–7116.
25. Kuna, J. J.; Voïtchovsky, K.; Singh, C.; Jiang, H.; Mwenifumbo, S.; Ghorai, P. K.; Stevens, M. M.; Glotzer, S. C.; Stellacci, F. The Effect of Nanometre-Scale Structure on Interfacial Energy. *Nat. Mater.* **2009,** *8*, 837–842.
26. Chandler, D. Physical Chemistry: Oil on Troubled Waters. *Nature* **2007,** *445*, 831–832.
27. Wang, Y.; Bhushan, B.; Zhao, X. Improved Nanobubble Immobility Induced by Surface Structures on Hydrophobic Surfaces. *Langmuir* **2009,** *25*, 9328–9336.
28. Janda, P.; Frank, O.; Bastl, Z.; Klementová, M.; Tarábková, H.; Kavan, L. Nanobubble-Assisted Formation of Carbon Nanostructures on Basal Plane Highly Ordered Pyrolytic Graphite Exposed to Aqueous Media. *Nanotechnology* **2010,** *21*, 095707.
29. Wang, Y.; Bhushan, B.; Zhao, X. Nanoindents Produced by Nanobubbles on Ultrathin Polystyrene Films in Water. *Nanotechnology* **2009,** *20*, 045301.
30. Fakhraai, Z.; Forrest, J. A. Measuring the Surface Dynamics of Glassy Polymers. *Science* **2008,** *319*, 600–604.
31. Torres, J. M.; Stafford, C. M.; Vogt, B. D. Manipulation of the Elastic Modulus of Polymers at the Nanoscale: Influence of UV−Ozone Cross-Linking and Plasticizer. *ACSNano* **2010,** *4*, 5357–5365.
32. Rouse, J. H.; Twaddle, P. L.; Ferguson, G. S. Frustrated Reconstruction at the Surface of a Glassy Polymer. *Macromolecules* **1999,** *32*, 1665–1671.
33. Zimmermann, R.; Freudenberg, U.; Schweiß, R.; Küttner, D.; Werner, C. Hydroxide and Hydronium Ion Adsorption—A Survey. *Curr. Opin. Colloid Interface Sci.* **2010,** *15*, 196–202.
34. Israelachvili, J. N. *Intermolecular and Surface Forces*, 2nd ed.; Academic Press: New York, 1991.
35. Grahame, D. C. The Electrical Double Layer and the Theory of Electrocapillarity. *Chem. Rev.* **1947,** *41*, 441–501.
36. Carruthers, J. C. The Electrophoresis of Certain Hydrocarbons and Their Simple Derivatives as a Function of pH. *Trans. Faraday Soc.* **1938,** *34*, 300–307.
37. Dickinson, W. The Effect of pH Upon the Electrophoretic Mobility of Emulsions of Certain Hydrocarbons and Aliphatic Halides. *Trans. Faraday Soc.* **1941,** *37*, 140–147.
38. Gray-Weale, A.; Beattie, J. K. An Explanation for the Charge on Water's Surface. *Phys. Chem. Chem. Phys.* **2009,** *11*, 10994–11005.
39. Zangi, R.; Engberts, J. B. F. N. Physisorption of Hydroxide Ions from Aqueous Solution to a Hydrophobic Surface. *J. Am. Chem. Soc.* **2005,** *127*, 2272–2276.
40. Liu, H.; Steigerwald, M. L.; Nuckolls, C. Electrical Double Layer Catalyzed Wet-Etching of Silicon Dioxide. *J. Am. Chem. Soc.* **2009,** *131*, 17034–17035.
41. Ang, P. K.; Chen, W.; Wee, A. T. S.; Loh, K. P. Solution-Gated Epitaxial Graphene as pH Sensor. *J. Am. Chem. Soc.* **2008,** *130*, 14392–14393.
42. Noah-Vanhoucke, J; Geissler, P. L. On the Fluctuations that Drive Small Ions toward, and away from, Interfaces between Polar Liquids and Their Vapors. *Proc. Natl. Acad. Sci. U.S.A.* **2009,** *106*, 15125–15130.
43. Kudin, K. N.; Car, R. Why Are Water-Hydrophobic Interfaces Charged?. *J. Am. Chem. Soc.* **2008,** *130*, 3915–3919.
44. Jungwirth, P.; Tobias, D. J. Molecular Structure of Salt Solutions: A New View of the Interface with Implications for Heterogeneous Atmospheric Chemistry. *J. Phys. Chem. B* **2001,** *105*, 10468–10472.
45. Schaffer, E.; Thurn-Albrecht, T.; Russell, T. P.; Steiner, U. Electrically Induced Structure Formation and Pattern Transfer. *Nature* **2000,** *403*, 874–877.

46. Seemann, R.; Herminghaus, S.; Jacobs, K. Dewetting Patterns and Molecular Forces: A Reconciliation. *Phys. Rev. Lett.* **2001,** *86*, 5534–5537.
47. Landau, L. D.; Pitaevskii, L. P.; Lifshitz, E. M. *Electrodynamics of Continuous Media*; Pergamon: New York; 1960.
48. The real field at the interface is likely to be larger than this conservative estimation: surface charge densities measured by titration of surfactant-free oil-in-water emulsions are typically 5 to 10 times larger[5] than the ones we estimate from streaming potential measurements.
49. The discontinuity in the normal component of the electric field and dielectric constant at the interface are at the origin of a nonzero normal component of the Maxwell tensor.
50. Killat, U. Revised Dynamical Theory of Thermoplastic Deformation. *J. Appl. Phys.* **1975,** *46*, 5169–5172.
51. Yang, Z.; Fujii, Y.; Lee, F. K.; Lam, C.-H.; Tsui, O. K. C. Glass Transition Dynamics and Surface Layer Mobility in Unentangled Polystyrene Films. *Science* **2010,** *328*, 1676–1679.
52. Siretanu, I.; Chapel, J.-P.; Drummond, C.; Procédé de Formation d'un Motif sur une Surface d'un Support. French patent application PCT/FR2011/000139.
53. Harrison, C.; Adamson, D. H.; Cheng, Z.; Sebastian, J. M.; Sethuraman, S.; Huse, D. A.; Register, R. A.; Chaikin, P. M. Mechanisms of Ordering in Striped Patterns. *Science* **2000,** *290*, 1558–1560.
54. Al Akhrass, S.; Ostaci, R.-V.; Grohens, Y.; Drockenmuller, E.; Reiter, G. Influence of Progressive Cross-Linking on Dewetting of Polystyrene Thin Films. *Langmuir* **2008,** *24*, 1884–1890.
55. Hunter, R. J. *Foundations of Colloid Science*; Oxford University Press, U.K., 1993; Vol. 1.